Amazon carbon emissions double mainly by dismantled in law enforcement

Luciana Gatti (lvgatti@gmail.com)
INPE - National Institute for Space Research https://orcid.org/0000-0003-4908-8974
Camilla Cunha
INPE - National Institute for Space Research
Luciano Marani
INPE - Instituto Nacional de Pesquisas Espaciais https://orcid.org/0000-0001-7382-464X
Henrique Cassol
National Institute for Space Research https://orcid.org/0000-0001-6728-4712
Cassiano Messias
INPE - National Institute for Space Research
Egidio Arai
INPE - Instituto Nacional de Pesquisas Espaciais
Luana Basso
National Institute for Space Research - INPE https://orcid.org/0000-0002-4208-6039
Luciana Soler
INPE - National Institute for Space Research
Claudio Almeida
INPE - National Institute for Space Research
Alberto Setzer
INPE - National Institute for Space Research
Lucas Domingues
IPEN
Scott Denning
Department of Atmospheric Science https://orcid.org/0000-0003-3032-7875
John Miller
NOAA https://orcid.org/0000-0001-8630-1610
Manuel Gloor
University of Leeds
Caio Correia
IPEN
Graciela Tejada
INPE - Instituto Nacional de Pesquisas Espaciais
Raiane Neves

INPE - Instituto Nacional de Pesquisas Espaciais
Raoni Rajão
Universidade Federal de Minas Gerais https://orcid.org/0000-0002-1133-4837
Felipe Nunes
Universidade Federal de Minas Gerais
Britaldo Soares-Filho
Universidade Federal de Minas Gerais
Jair Schmitt
Universidade Federal de Minas Gerais
Carlos Nobre
University of São Paulo
Sergio Correa
UERJ - Rio de Janeiro State University https://orcid.org/0000-0002-0038-0790
Alber Sanchez
National Institute for Space Research https://orcid.org/0000-0001-7966-2880
Luiz Aragão
National Institute for Space Research
Liana Anderson
CEMADEN https://orcid.org/0000-0001-9545-5136
Celso von Randow
National Institute for Space Research https://orcid.org/0000-0003-1045-4316
Stephane Crispim
INPE - Instituto Nacional de Pesquisas Espaciais
Francine Silva
INPE - National Institute for Space Research
Guilherme Machado
INPE - National Institute for Space Research

Physical Sciences - Article

Keywords:

Posted Date: September 19th, 2022

DOI: https://doi.org/10.21203/rs.3.rs-2023624/v1

Amazon carbon emissions double mainly by dismantled in law enforcement

Luciana V. Gatti[1,2*], Camilla L. Cunha[1], Luciano Marani[1], Henrique L. G. Cassol[1], Cassiano Gustavo Messias [1], Egidio Arai[1], Luciana Soler[1], Claudio Almeida[1], Alberto Setzer[1], Luiz E. O. C. Aragão[1], Luana S. Basso[1], Lucas Gatti Domingues[2,3], A. Scott Denning[4], John B. Miller[5], Manuel Gloor[6], Caio S. C. Correia[1,2], Graciela Tejada[1], Raiane A. L. Neves[1], Raoni Rajao[7], Felipe Nunes[7], Britaldo S.S. Filho[7], Jair Schmitt[7], Carlos Nobre[8], Sergio M. Corrêa[9], Alber H. Sanches[1], Liana Anderson[10], Celso Von Randow[1], Stephane P. Crispim[1], Francine M. da Silva[1], Guilherme B.M. Machado[1]

[1]General Coordination of Earth Science (CGCT), National Institute for Space Research (INPE), São José dos Campos, Brazil.

[2]Nuclear and Energy Research Institute (IPEN), São Paulo, Brazil.

[3]National Isotope Centre, GNS Science, Lower Hutt, New Zealand

[4]Colorado State University;

[5]Global Monitoring Laboratory, National Oceanic and Atmospheric Administration (NOAA), Boulder, CO, USA

[6]University of Leeds, School of Geography, Leeds, UK;

[7]Universidade Federal de Minas Gerais;

[8]USP – University of São Paulo, IEA, São Paulo, Brazil;

[9]Rio de Janeiro State University (UERJ), Resende, Brazil;

[10]CEMADEN, São José dos Campos, Brazil;

*luciana.gatti@inpe.br or lvgatti@gmail.com

Summary

The Amazon Forest is a major locus for carbon and water cycling in the climate system whose function has been degraded in recent decades by land use and climate change. Most studies of Amazonia's carbon balance have been limited by sparse sampling. We measured 742 atmospheric vertical profiles of CO_2 and CO over four regions of Amazonia from 2010 through 2020. We estimate that Amazon carbon emissions increased from 0.24±0.19 PgC y^{-1} in 2010-18 to 0.44±0.22 in 2019 and 0.52±0.22 PgC y^{-1} in 2020. During these years, increases were also observed in deforestation (79% and 74%) and forest burned area (14% and 42%). Field notifications for illegal deforestation and related crimes dropped by 42%, while fines paid for judgments held fell by 89%. Carbon losses during 2019 and 2020 were comparable to losses in the record warm El Nino event of 2015-16, but this time with usual to moderate Oceanic Ninõ Index. 2020 showed 12% decrease in precipitation indicating also a climate impact in carbon emissions. The changes during 2019 and 2020 were mainly due to the western Amazonia becoming also a carbon source. We hypothesize that the consequences of the collapse in enforcement led to increase in deforestation, biomass burning and degradation producing net carbon losses and enhancing drying and warming of forest regions.

Introduction

The Amazon hosts the largest tropical forest on the planet and has proven to be an important carbon sink in the recent past[1–3]. This carbon sink is declining, mainly due to increased tree mortality[1] as a result of deforestation and climate change[4]. The Amazon Forest represents around 50% of the global tropical rainforest and contains about 90 Pg C in above and below ground vegetation biomass[5,6], which can be quickly released and can thus result in substantial positive feedback on global climate[7]. Furthermore, deforestation and forest degradation reduce the forest´s capability to act as a carbon sink[1–3,8].

In the Amazon the relationships between ecosystem carbon and water cycles, and climate are complex. Several studies have estimated that evapotranspiration is responsible for up to 50% of water recirculation in Amazonian precipitation[9]. Hydrologically, the Amazon is one of the three main air upwelling regions in the tropics and rainfall in the whole basin, averaging about 2,200 mm per year[10]. Large-scale human disturbance alters these ecosystem-climate interactions. In the last 40 to 50 years, human impact has increasingly affected Amazonia, resulting in a forest loss of around 18%, of which 14% has been converted mainly to agricultural land (89% pastures and 10% crops)[3].

Over the past two three years illegal deforestation has strongly increased in parallel to changes in governance. We analyze how these changes affect the Amazonian carbon balance and how they are linked to deforestation and fire feedbacks. Forest removal reduces evapotranspiration and rainfall while increasing temperature[9,11–14]. Additionally, regional deforestation followed by fires and selective logging causes degradation of adjacent forests, increasing the vulnerability to fires. Regional and global warming are synergistic and mutually reinforcing.

We compared the mean Amazonian carbon balance over 9 years (2010-18)[4] with the subsequent two years when reduction in public policies to control deforestation was intense, using deforestation data analysis to georeferenced the carbon sources (limited to the Brazilian Amazon – PRODES[15]), incidence of fire spots (Pan-Amazônia)[16] and burned area, and, pointing out the main factors responsible for the conversion of Amazonia into a carbon source.

Atmospheric carbon vertical profiles

We performed 742 vertical profiles (VPs) from 2010 to 2020, using small aircraft over 4 Amazon sites, representing large upwind regions (Extended Data Fig. 1), where the VPs reflect the result of all carbon sources and sinks processes between the Brazilian Atlantic coast and the VP sites[4,17,18]. As in past studies, the VP sites were SAN (northeast region: 2.86° S 54.95° W), ALF (southeast region: 8.80° S 56.75° W), RBA (southwest region: 9.38° S 67.62° W), and in the northwest region TAB (northwest region: 5.96° S 70.06° W); from 2013 in TEF (3.39° S 65.6° W)[5]. The sampling frequency was approximately 2 times per month in each location, from 4.4 km height (a.s.l.) to close to the surface, and usually carried out between 12:00 and 13:00 local time. The CO_2 and CO samples were analysed at INPE's LaGEE (Greenhouse Gas Laboratory), in São Jose dos Campos.

To construct the annual mean vertical profile enhancements (ΔVP) for each site (Extended Data Fig. 2), we subtracted the specific background (bkg) for each flask (height), from each VP, and then calculated the monthly mean enhancement per height and per year. This study extends results and analysis of ΔVP for the years 2019 and 2020. We present the weighted mean all-Amazonia vertical profile (Figure 1) based on regions of influence for each site per year, which represents an advance over the previous study[4] (see methods). The ΔVP are a large scale ecosystem functioning indicator and strongly related to the carbon budget. In Figure 1 we present the Amazonian annual mean ΔVP from 2010 to 2020, presenting the mean 2010-18 to highlight the years 2019 and 2020 compared to the previous mean. We observed net positive CO_2 contribution to the atmosphere for the ΔVP mean 2010-18 of 0.24 ppm. This indicates that Amazonia is a carbon source to the atmosphere, considering all natural and anthropogenic processes of CO_2 emissions and absorptions. This result is indicative if the Amazonia contribution as a sink or source in the global carbon budget, as there are well known discrepancies from many studies using different methodologies (bottom-up, top-down techniques, and a wide variety of global, regional and inversion models)[1–4,8,19–23].

Comparing Amazonian mean ΔVP in 2019 and 2020 with the mean for 2010-18, we observed an increase of 50% and 142%, respectively. This strong and rapid increase in concentration gradient represents a similarly strong increase in total carbon emissions and coincides with strong increases in deforestation. According to PRODES[8], deforestation in the Brazilian

Amazon increased by 79% and 74% for the years 2019 and 2020 compared with the mean for 2010-18 (Figure 2, Extended data Fig. 3a,c). For the same period and comparison, considering the whole Amazonia, burned area by MODIS (collection 6, see methods) increased 14% in 2019 and 42% in 2020 (Extended data Table 1). Fire spots from INPE[16] were used to map fire distribution in Amazonia and were underestimated compared with burned area (see methods). Fire spots increased 3% in 2019 and 22% in 2020 relative to the previous period (Extended Data Fig. 3b,c & 4a). There were alarming increases in wood exports and the area of corn and soybean plantations in 2019-2020. Cattle populations have decreased in Brazilian states outside of Amazonia but increased very intensely in the Amazonia (Extended Data Fig. 5a,b), indicating the drivers of deforestation[24–26].

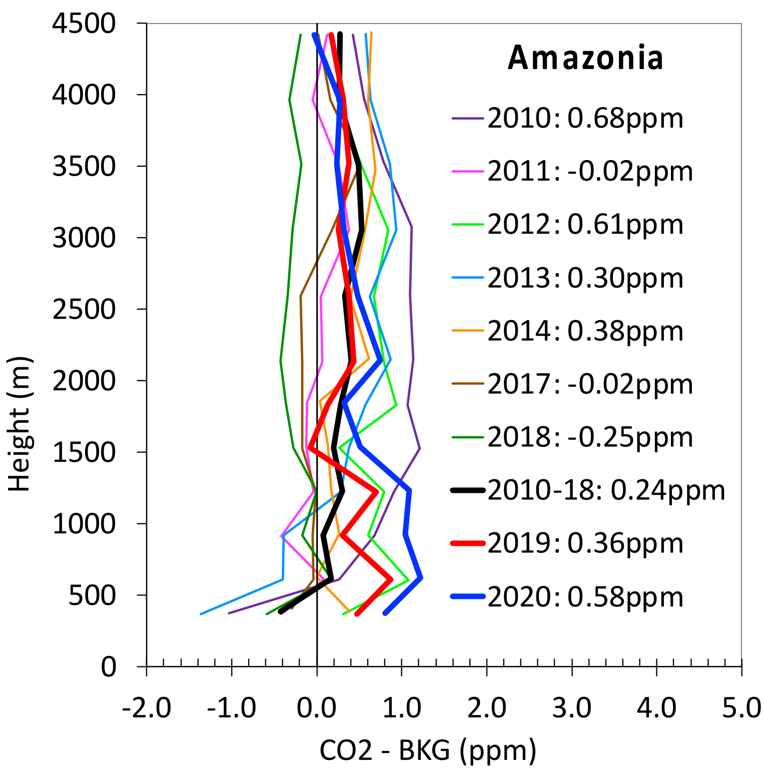

Figure 1 | Amazonia Annual Mean Vertical Profiles. Amazonia annual means vertical profile for each year (2010-2020), except 2015 and 2016, because are not complete for all 4 sites, constructed from vertical profile monthly mean (each height was subtracted by the background) producing (ΔVP). The mean for each height using the 4 sites reproduced by the same methodology used for the Amazonia mean flux, separating Amazonia in 3 regions (see methods and Extended data Fig. 1b). The black thick line represent the 2010-2018 Amazonia mean vertical profiles, the red thick line 2019 mean and blue thick line 2020 mean. ΔVP annual mean for each site and each year are show in Extended Data Fig 2.

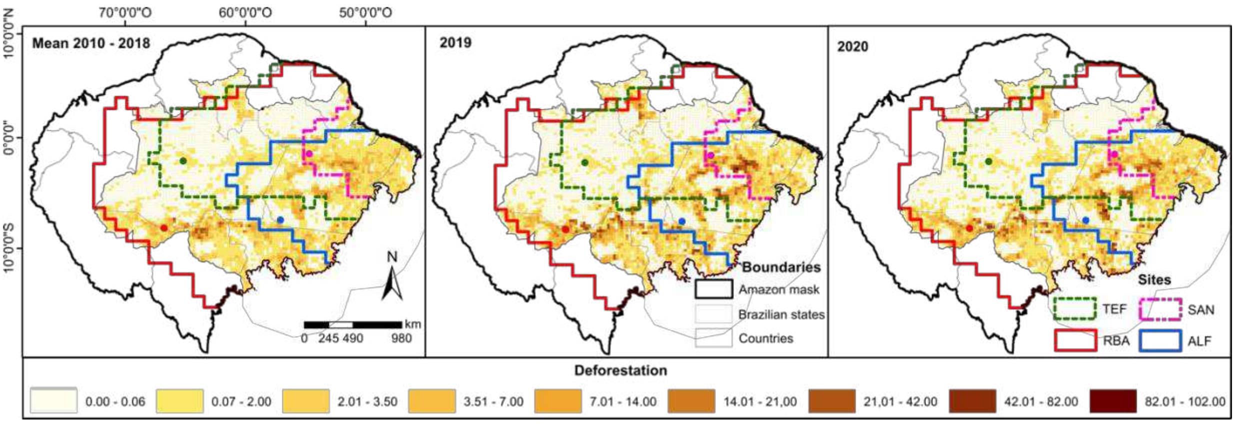

Figure 2 | Amazon deforestation map. Deforestation area (km^2) maps are given limited in Brazilian Amazonia in grid cells of 0.25˚x0.25˚ by PRODES[27]. The mean deforestation area per grid between 2010-18 (left); Absolute deforested area in 2019 (centre); Absolute deforested area in 2020 (right). Deforestation maps are given in grid cells were the increment (left) or the absolute deforested area (centre, right), are composed by polygons higher than 0.0625 km^2, and are given in deforested km^2 per grid cell.

After the revision of the Forest Code in 2012[28], deforestation in the Brazilian Amazonia has risen gradually culminating in 2021 with the highest annual rate since 2006. This upsurge in deforestation rates along with higher carbon emissions follows the dismantling of federal environmental agencies in charge of law enforcement in the region, especially after 2018, when field notifications and judgments resulting in fines paid reached the lowest number on record over the last decade (Figure 3). From 2010 to 2018, an annual mean of 4734 infraction notices were filed in the Amazonia for violations against flora (mostly illegal deforestation). In 2019 it reduced to 3331 and in 2020 to 2193 representing a reduction of 30% and 54%, respectively. In addition, the annual mean of judgments and the respective number of fines paid up to the subsequent year dropped by 74% and 89%, respectively, contributing to an increased sense of impunity across the region (see additional analysis of environmental law enforcement in Supplementary Information 1).

Regional Amazonian Carbon Fluxes

We calculate total carbon flux (FC_{Total}) using a column budget technique (see methods). FC_{Total} is the sum of all natural and anthropogenic carbon sink and sources between the coast and aircraft vertical profiles sites[4]. Using identical methods, CO was used to determine the fraction of FC_{Total} come from biomass burning (FC_{Fire}), where we used a mean ratio CO:CO_2 specific for each site (see methods). The residual between total carbon and fire flux is designated Net Biome Exchange (NBE). The FC_{NBE} includes photosynthesis, respiration, decomposition and other non-fire anthropogenic emissions. Decomposition can come from natural process but also from land use change and degradation[29] (all emissions following fire). From 2010 to 2018 FC_{Total} was 0.09±0.08 gC m^{-2} d^{-1}, equivalent to 0.25±0.19 PgC y^{-1}, considering Amazonian area of 7,256,362 km^2. In 2019 the calculated FC_{Total} indicated an enhancement of 89% in total carbon emissions (0.17±0.09 gC m^{-2} d^{-1}; 0.44±0.22 PgC y^{-1}) and in 2020 a greater increase of 122% (0.20±0,09 gC m^{-2} d^{-1}; 0.52±0.22 PgC y^{-1}) relative the 2010-18 mean (Figure 4a,b).

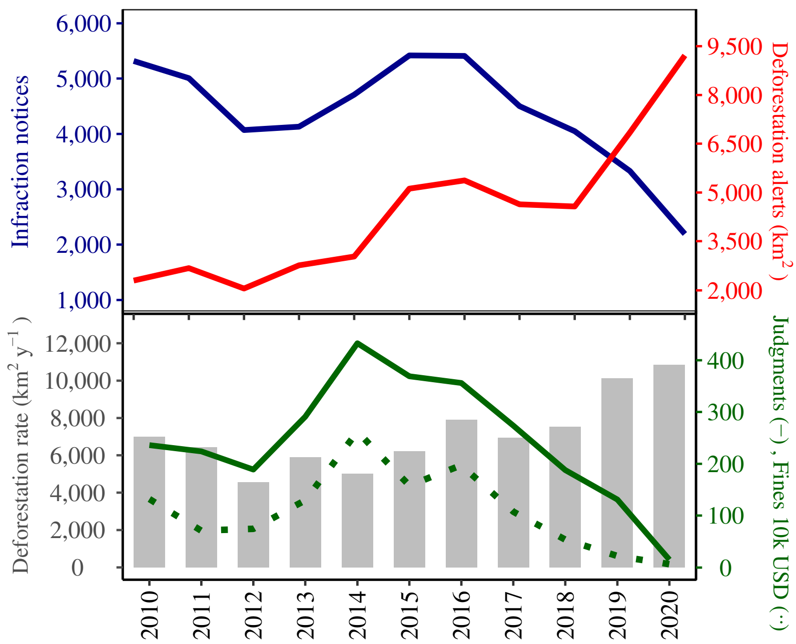

Figure 3 | Environmental law enforcement and accountability for crimes against Amazon Forest. a) number of infractions against flora issued by IBAMA and deforestation alerts by INPE in support of IBAMA´s environmental field operations (Deter-Modis and Deter-B). An infraction notice informs citizens, companies, or institutions about committed acts violating administrative rules or the law, which are subject to penalties such as fines, seizures, and embargoes after due administrative judgments. b) number of administrative judgments of infraction notices against flora and the amount of fines paid by the following year from the judgment. Monetary values were adjusted for inflation and converted to USD using a rate of R$ 5 (Brazilian Reais) per U.S.$ 1.

Amazonia total carbon emissions in 2019 and 2020 were comparable to carbon losses during the extreme El Nino event of 2015/16 (Figure 4), during which the rate of growth of atmospheric CO_2 was one of the highest ever measured[30–32] . In 2019, 3 months of weak El Niño (maximum +0.7 indices /warm) were observed during wet season, increases in deforestation by 79% and in burned area by 14%, but with climatological conditions similar to the 2010-18 period. In 2020 during the dry season a moderate La Nina (maximum -1.3 /cold)[33] was observed (Extended Data Fig. 6 and Supplementary Fig. 2). The resultant of 122% increase in carbon emissions in 2020 is the combination of increase in 74% of deforestation and 42% in burned area, and reduction of 12% in annual precipitation. The reduction was mainly during wet season (January, February and March loss of 26%) and the temperature in the same period increased by 0.6˚C (Extended data Table 1 and Extended data Fig. 6). Precipitation losses in the wet season will impact carbon emissions mainly during dry season, when water availability will be lower to the forest. Figure 2a, b and c present the strong increase in deforestation in 2019 and 2020 in some regions in Brazilian Amazonia and Figure 4 (CF_{Total}) and Extended Data Fig. 7 (FC_{Fire} and NBE) show the seasonality and interannual variability in carbon emissions, where Fig. 4b shows the similar magnitude in carbon emissions for 2019 and 2020, but without the extreme El Ninõ during 2010, 2015/2016. To evaluate the trend of Amazon carbon emissions we separated the 11 years' time series into two groups of five years: 2010-14 and 2016-20.

Seasonal carbon fluxes integrated across Amazonia show that the increase happens mainly during the dry season in both years (Fig. 4). Fire emissions calculated by our method (FC_{Fire}) show a mean 2010-18 emission rate of 0.15±0.02 gC m^{-2} d^{-1} (0.40±0.04 PgC y^{-1}) with 8% and 4% increases during 2019 and 2020, respectively (Extended Figure 7a,c). The larger increases in total carbon emissions across Amazonia during these years come mainly from NBE, where the mean 2010-18 (FC_{NBE}) was a -0.06±0.07 gC m^{-2} d^{-1} (-0.15±0.19 PgC y^{-1}), in 2019 was +0.01±0.08 gC m^{-2} d^{-1} and 2020 was +0.05±0.08 gC m^{-2} d^{-1}, representing near carbon neutrality for forest (excluding fire) for the last 2 years of this time series. As we are using a fixed $CO:CO_2$ ratio for each site and we know that the driest forest will be more flammable, we need to consider the possibility that a fraction of fire emissions may also have been incorporated into the NBE, as we observe its variability from month by month and year by year, depending on climate conditions[4]. Uncertainties and variability in $CO:CO_2$ ratios used to calculate FC_{Fire} may help explain the discrepancy between the near-absence of FC_{Fire} anomalies in the 2019-2020 period and the clear anomalies in fire hot spots and burned area. The fact that NBE represents the largest increase indicates that the forests carbon sink was lower than the emissions from natural and anthropogenic process (deforestation and degradation) as we measure in the atmosphere. Regardless of whether it is enhanced respiration or fire associated with deforestation and degradation, our FC_{Total} results clearly show that Amazonia is emitting more carbon, amplifying the consequence of global climate[4].

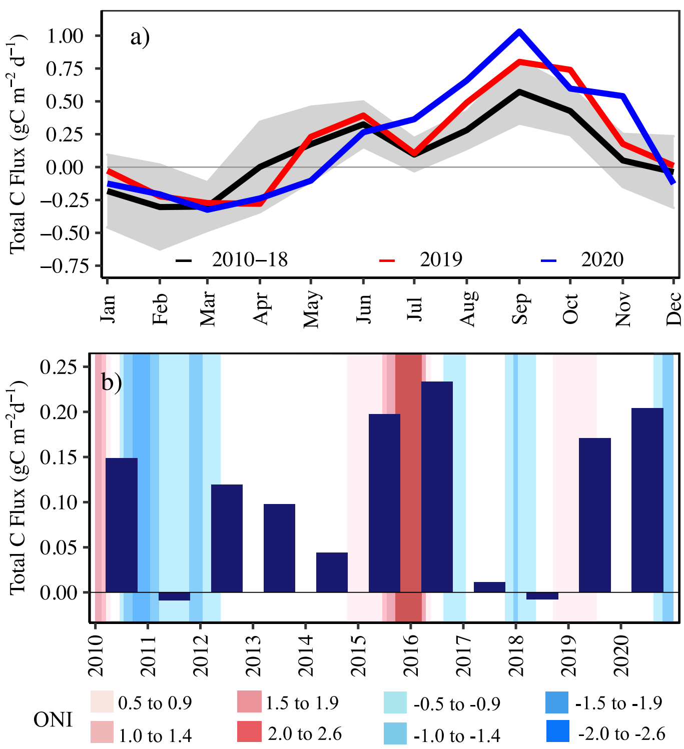

Figure 4 | Amazonia carbon flux 2010-20. a) Seasonal Amazonia total carbon flux (FC_{Total}). Black line for 2010-18 mean, where grey bands denote the standard deviation of the monthly mean. Red line shows the seasonal FC_{Total} for 2019 and blue line for 2020. b) Annual mean Amazonia total carbon flux blue bar and the ONI classification in the background showing El Niño and La Niña (see Extended Data Fig. 6a and methods).

Impact of deforestation and climate change per region

Seasonal and interannual variability of component carbon fluxes, ΔVP and related studied parameters for each region are presented in Extended Data Table 1 and Extended Data Figs. 2, 8, 9 and seasonal fluxes for all sites are presented in the Supplementary Fig. 3.

SAN, in the northeast, is the region most impacted by deforestation and precipitation reduction, mainly during the dry season. The region influencing the vertical profiles was 36% deforested, with a 67% increase in deforestation in 2019 and a 45% increase in 2020 relative to the 2010-2018 period. 2019 compared with the 2010-18 mean exhibits a very unusual reduction of 42% in precipitation during the wet season peak of JFM (Jan, Feb, Mar) and an annual increase of 78% in total carbon emissions (from 0.36±0.13 to 0.64±0.17 $gCm^{-2}d^{-1}$), due to an increase in a carbon source in FC_{NBE}. All fluxes for all sites, deforestation, burned area, precipitation and temperature are presented in Extended data Table 1. In 2020, deforestation increased in this region by 45%, but 2020 was the second year with fire reductions and more stable climate conditions resulting in nearly the same carbon emissions as the 2010-18 mean (6% decrease) and near neutrality for FC_{NBE}. Comparing 5 year mean carbon budgets for the first part of time series (2010-2014) and second part (2016-2020) we observe a reduction of 31% for total carbon emissions, a reduction of 20% in burned area, an increase in 23% of deforestation, a decrease in annual accumulated precipitation of 6% (decrease in 12% JFM and 20% ASO) and an increase of 0.4˚C in temperature during the peak of dry season (Aug-Sep-Oct) promoting more climate stress to the remaining forest. The reduction in fire emissions for this region explain most of the reduction in FC_{Total}.

The southeast (represented by ALF) was the second most impacted region and was 29% deforested, and the deforestation increased 80% in 2019 and 87% in 2020 relative to the 2010-

18 mean. Total carbon emission in 2019 was similar to the mean 2010-18, but increased 53% in 2020. Burned area and FC_{Fire} increased by 28% and 24%, respectively in 2020, while precipitation in the region decreased (JFM ↓27% and ASO ↓20%) and temperature during JFM increased by 0.5˚C, promoting climate stress, reducing carbon sink and increasing emissions. Net biome exchange increased in emissions 111% during 2020 (from 0.09±0.05 to 0.19±0.05 gC m^{-2} d^{-1}). Comparing 5 year means between the earlier (2010-14) and later periods (2016-20) we observed an increase of 77% in the FC_{Total}, stable fire emissions and an increase in carbon losses (from 0.02±0.05 to 0.17±0.05 gC m^{-2} d^{-1}) in FC_{NBE}. Deforestation increased 46%, burned area increased 22%, annual precipitation decreased 77mm (4%), where 39mm was during JFM (↓12%) and temperature increased 0.9˚C during the same period of JFM. The wet season represents the main carbon sink time whereas during dry season the climate conditions are less favourable across Amazonia's southeast.

RBA in the southwest region, currently 17% deforested, was near carbon neutral during the period 2010-18, and continued to be in 2019, but in 2020 total carbon emissions (FC_{Total}) increased leaving the condition of carbon neutrality (from 0.04±0.04 to 0.16±0.05 gC m^{-2} d^{-1}), mainly because FC_{NBE} became neutral. Deforestation increased 81% in 2019 and 76% in 2020 relative to 2010-18 and burned area increased 5% and 3%. Precipitation during 2020, related to the 2010-18 mean, dropped by 18% in the annual mean, 41% during JFM and 15% in ASO, and temperature also increased 0.8˚C during JFM. These stress conditions in 2020 may be a consequence of the strong increase of deforestation impacting evapotranspiration and temperature. Physiological stresses impact the forest flammability, promoting more fires, degradation and reducing the carbon sink. Comparing 5 year means for the two periods (2010-14 and 2016-20) we observed an increase of 59% in FC_{Total} and 39% in FC_{Fire} confirming this tendency. FC_{NBE} increased 31%, but in the last year 2020 changed from sink to neutral for

NBE. Deforestation and burned areas increased and affected preserved regions in the west part of Amazonia. Across the State of Amazonas, a strong increase in deforestation (Extended Data Fig. 4c) and in fire spots was observed (93% July and 92% August 2019 and 199% July and 131% August 2020).

The least human-impacted northwest region (TAB_TEF), currently 15% deforested, exhibited a near neutral carbon budget for the period 2010-18, but in 2019 became a carbon source (FC_{Total}) showing the total carbon flux increased more than tenfold and fivefold in 2020 (from 0.02±0.05 to 0.21±0.06 and 0.11±0.06 gC m^{-2} d^{-1}, respectively). The main reason was that NBE became a carbon source. In 2019 and 2020, deforestation increased by 95% and 73% relative to the previous period. In 2019 during the months February to April a large area was burned in Roraima state (upwind from the sample site), north of the equator, where those months are the dry season (Extended data Fig. 4a,b) with increases of fire spots of 435% and 718% during March April, respectively. A reduction of 23% in precipitation during the peak of wet season (JFM) in 2019 and 42% during 2020, and temperature also increased up to 0.5˚C for the same period. Comparing the two 5 years mean in our time series (2010-14 and 2016-20) we observed a trend of increase in FC_{Total} (from 0.02±0.05 to 0.06±0.04 gC m^{-2} d^{-1}), 25% at FC_{Fire}, and 34% reduction in carbon uptake in FC_{NBE} showing a tendency toward reduction in the carbon sink. Deforestation increased 48%, annual precipitation decreased 8% (191mm) with a 29% decrease during JFM and a decrease of 4% in ASO. The annual temperature increased 0.4˚C and 0.8˚C in ASO.

Over the past 40 years, deforestation and global warming have been accompanied by reduced precipitation and warmer temperatures have made the dry season drier, hotter, and longer[4]. This shift promotes stress conditions in the forest[13]. These conditions imply a strong stress for the trees, providing an imbalance between photosynthesis and respiration, increasing the flammability of the trees, which produces an intensification of degradation in these regions, as fire penetrates more and more in preserved forests areas. This process appears to have intensified since 2018. We estimate that carbon emissions doubled in the years 2019 and 2020, compared with the previous study (2010-18), because of a reduction of law enforcement in Brazilian Amazonia, resulting in an important increase in deforestation during 2019 and in 2020 the climate stress was also an additional cause for carbon source.

Comparing the mean for 2010-14 with the 2016-20 for the whole Amazonia, we observed 50% increase in total carbon emissions (FC_{Total} 0.21±0.07 PgC y^{-1} and 0.31±0.07 PgC y^{-1}, respectively), 31% decrease in carbon sink (FC_{NBE} -0.15±0.07 PgC y^{-1} and -0.10±0.07 PgC y^{-1}, respectively) and 16% increase in fire emissions (FC_{Fire}. 0.36±0.02 PgC y^{-1} and 0.42±0.02 PgC y^{-1}, respectively This consistent increase in the last 5 years was accelerated in the last 2 years of the period, showing the importance of public policies to prevent deforestation, degradation and fire occurrences. Zero deforestation and forest restoration will be very important to reduce this climate stress, which is amplified by global climate change, resulting in decreased carbon sink capacity, as well as increased carbon emissions from Amazonia and the impact on the water cycle.

References

1. Brienen, R. J. W. *et al.* Long-term decline of the Amazon carbon sink. *Nature* **519**, 344–348 (2015).
2. Phillips, O. L. & Brienen, R. J. W. Carbon uptake by mature Amazon forests has mitigated Amazon nations' carbon emissions. *Carbon Balance Manag.* **12**, 1 (2017).
3. Hubau, W. *et al.* Asynchronous carbon sink saturation in African and Amazonian tropical forests. *Nature* **579**, 80–87 (2020).
4. Gatti, L. V. *et al.* Amazonia as a carbon source linked to deforestation and climate change. *Nature* **595**, 388–393 (2021).

5. SAATCHI, S. S., HOUGHTON, R. A., DOS SANTOS ALVALÁ, R. C., SOARES, J. V. & YU, Y. Distribution of aboveground live biomass in the Amazon basin. *Glob. Chang. Biol.* **13**, 816–837 (2007).
6. Malhi, Y. *et al.* Chapter 6: Biogeochemical Cycles in the Amazon. in *Amazon Assessment Report 2021* (UN Sustainable Development Solutions Network (SDSN), 2021). doi:10.55161/TAKR3454
7. Cox, P. M., Betts, R. A., Jones, C. D., Spall, S. A. & Totterdell, I. J. Acceleration of global warming due to carbon-cycle feedbacks in a coupled climate model. *Nature* **408**, 184–187 (2000).
8. Aragão, L. E. O. C. *et al.* 21st Century drought-related fires counteract the decline of Amazon deforestation carbon emissions. *Nat. Commun.* **9**, (2018).
9. Costa, M. H. *et al.* Chapter 7: Biogeophysical Cycles: Water Recycling, Climate Regulation. in *Amazon Assessment Report 2021* (UN Sustainable Development Solutions Network (SDSN), 2021). doi:10.55161/KKHX1998
10. *Amazon Assessment Report 2021*. (UN Sustainable Development Solutions Network (SDSN), 2021). doi:10.55161/RWSX6527
11. Costa, M. H. & Pires, G. F. Effects of Amazon and Central Brazil deforestation scenarios on the duration of the dry season in the arc of deforestation. *Int. J. Climatol.* **30**, 1970–1979 (2010).
12. Leite-Filho, A. T., Costa, M. H. & Fu, R. The southern Amazon rainy season: The role of deforestation and its interactions with large-scale mechanisms. *Int. J. Climatol.* **40**, 2328–2341 (2020).
13. Leite-Filho, A. T., Soares-Filho, B. S., Davis, J. L., Abrahão, G. M. & Börner, J. Deforestation reduces rainfall and agricultural revenues in the Brazilian Amazon. *Nat. Commun.* **12**, 2591 (2021).
14. Leite-Filho, A. T., de Sousa Pontes, V. Y. & Costa, M. H. Effects of Deforestation on the Onset of the Rainy Season and the Duration of Dry Spells in Southern Amazonia. *J. Geophys. Res. Atmos.* **124**, 5268–5281 (2019).
15. Almeida, C. A., Maurano, L. E. P., Valeriano, D. D. M., Camara, G., Vinhas, L., Gomes, A. R., Monteiro, A. M. V., Souza, A. A. A., Renno, C. D., Silva, D. E., Adami, M., Escada, M. I. S., Mota, M., Kampel, S. A. Methodology for Forest Monitoring used in PRODES and DETER projects. *INPE, version: 2021-01-26. IBI: <8JMKD3MGP3W34R/443H3RE>* (2021). Available at: http://urlib.net/rep/8JMKD3MGP3W34R/443H3RE. (Accessed: 25th April 2021)

16. BDQueimadas. INPE Biomass burning Program. (2022). Available at: https://queimadas.dgi.inpe.br/queimadas/bdqueimadas.
17. Basso, L. S. *et al.* Amazon methane budget derived from multi-year airborne observations highlights regional variations in emissions. *Commun. Earth Environ.* **2**, 246 (2021).
18. Gatti, L. V. *et al.* Drought sensitivity of Amazonian carbon balance revealed by atmospheric measurements. *Nature* **506**, 76–80 (2014).
19. Gatti, L. V *et al.* Cross Chapter 1: The Amazon Carbon Budget. in *Amazon Assessment Report 2021* (UN Sustainable Development Solutions Network (SDSN), 2021). doi:10.55161/VNBV7494
20. Silva Junior, C. H. L. *et al.* Persistent collapse of biomass in Amazonian forest edges following deforestation leads to unaccounted carbon losses. *Sci. Adv.* **6**, eaaz8360 (2020).
21. Aguiar, A. P. D. *et al.* Land use change emission scenarios: anticipating a forest transition process in the Brazilian Amazon. *Glob. Chang. Biol.* **22**, 1821–1840 (2016).
22. Assis, T. O. *et al.* CO2 emissions from forest degradation in Brazilian Amazon. *Environ. Res. Lett.* **15**, 104035 (2020).
23. Feng, L. *et al.* Consistent regional fluxes of CH4 and CO2 inferred from GOSAT proxy XCH4:XCO2 retrievals, 2010–20. *Atmos. Chem. Phys.* **17**, 4781–4797 (2017).
24. IBGE Statistics- Brazilian Institute of. Agriculture, Livestock and others. (2022). Available at: https://www.ibge.gov.br/estatisticas/economicas/agricultura-e-pecuaria/9117-producao-agricola-municipal-culturas-temporarias-e-permanentes.html?t=series-historicas. (Accessed: 11th July 2022)
25. MDIC, B. G.-. Comexstat. Available at: http://comexstat.mdic.gov.br/pt/comex-vis. (Accessed: 11th July 2022)
26. Geography, I. S.-B. I. of. Cattle. Available at: https://sidra.ibge.gov.br/tabela/3939#resultado. (Accessed: 11th July 2022)
27. PRODES. Amazon Deforestation Monitoring Project (PRODES / INPE). (2022). Available at: http://www.obt.inpe.br/OBT/assuntos/programas/amazonia/prodes.
28. Soares-Filho, B. *et al.* Cracking Brazil's Forest Code. *Science (80-.).* **344**, 363–364 (2014).
29. Aragão, L. E. O. C. *et al.* Environmental change and the carbon balance of Amazonian forests. *Biol. Rev.* **89**, 913–931 (2014).
30. Global Monitoring Laboratory. Trends in Atmospheric Carbon Dioxide. Available at: https://gml.noaa.gov/ccgg/trends/gl_gr.html.
31. Gloor, E. *et al.* Tropical land carbon cycle responses to 2015/16 El Niño as recorded by

atmospheric greenhouse gas and remote sensing data. *Philos. Trans. R. Soc. B Biol. Sci.* **373**, 20170302 (2018).

32. Withey, K. *et al.* Quantifying immediate carbon emissions from El Niño-mediated wildfires in humid tropical forests. *Philos. Trans. R. Soc. B Biol. Sci.* **373**, 20170312 (2018).
33. Weather, N. O. and A. A. (NOAA) / N. W. S. / C. &. Oceanic Niño Index (ONI). (2022). Available at: https://origin.cpc.ncep.noaa.gov/products/analysis_monitoring/ensostuff/ONI_v5.php. (Accessed: 7th May 2022)

Acknowledgements This work was funded by many projects from the long term measurements: State of Sao Paulo Science Foundation - FAPESP (16/02018-2, 11/51841-0, 08/58120-3, 18/14006-4, 18/14423-4, 18/18493-7, 19/21789-8, 11/17914-0), UK Environmental Research Council (NERC) AMAZONICA project (NE/F005806/1), NASA grants (11-CMS11-0025, NRMJ1000-17-00431), 7FP EU (283080), MCTI/CNPq (2013), CNPq (134878/2009-4), ERC / Horizon 2020 (649087) coordinated by Wouter Peters. We thank numerous people at NOAA/GML who provided advice and technical support for air sampling and measurements in Brazil and the pilots and technical team at aircraft sites who collected the air samples. We thank J. F. Mueller for providing modelled biogenic CO fluxes.

Author Contributions LVG, MG, JM conceived the basin-wide measurement program and approach; LVG wrote the paper; all co-authors participated in many scientific meetings to produce and interpreted the data, commented and review the manuscript; LGD, AS, LSB, HC, GT, LM, LVG contributed with region of influence study; HC, EA, CLC, LM, LVG, LSB, SMC contributed with climate data weighted studies; CGM, LS, CA, AS, GT contributed with deforestation and fire spots analysis, LGD, CC, SC, RL, FMS, GBMM contributed with GHG concentration analysis; RR, FN, BSSF, JS contributed with law enforcement analysis, SB, JM, LVG contribute with estimate of the biogenic CO.

Author Information Reprints and permissions information is available at npg.nature.com/reprints and permissions. The authors declare no competing financial interests. Correspondence and requests for materials should be addressed to LVG (luciana.gatti@inpe.br or lvgatti@gmail.com).

Additional Information Extended Data and Supplementary Information is available for this paper

Methods

Sites, air sampling and analysis

Here we are reporting the results from measurements at the four Amazonian aircraft vertical profile sites of the CARBAM project (SAN: 2.86° S 54.95° W; ALF: 8.80° S 56.75° W; RBA: 9.38° S 67.62° W; in 2010-2012 for TAB: 5.96° S 70.06° W; and since 2013 for TEF; 3.39° S 65.6° W) for 2019 and 2020, in addition to the measurements between 2010 and 2018 detailed at Gatti et al.[4]. Our samples were done typically twice per month, resulting in approximately 742 vertical profiles over these 11 years, in a descending spiral profile from 4,420 m to 300 m above sea level (a.s.l.). In 2015 the data collection flights were stopped in April at all sites, returning in November at RBA. In 2016, profiles were performed only at RBA and ALF. The VPs were usually taken between 12:00 and 13:00 local time. Air samples were analysed by a non-dispersive infrared analyser for CO_2 and by gas chromatography with HgO reduction detection for CO. The detailed analytical and sampling methods were presented in previous studies[4,18]. We defined the Amazon study area similarly to Gatti et al.[4], according to subregions from Eva et al.[34] and biomes from Olson et al.[35], where the studied area in the Amazonia was determined considering forest ecosystems sub-regions: Amazônia stricto sensu, Guianas, Andes and Gurupi, with a total area of 7,256,362 km^2 [4].

Annual Mean Vertical Profiles. The annual mean ΔVP for each site was calculated starting with individual profiles where for each altitude (sampled flask) the CO_2 concentration was subtracted from the correspondent background (bkg), then averaging first to monthly and later to annual mean by height (Extended Data Fig. 2). To calculate the annual mean Amazonia vertical profile, we apply the same method used to obtain the mean Amazonia flux. To scale for the whole Amazonia, we separated Amazonia in 3 regions (Extended Data Fig 1b). To compose the ΔVP Region 1 (SAN + ALF) the weighted mean concentration of CO_2 minus bkg was produced for each height, proportional to the respective areas. The compose the ΔVP Region 2 (RBA + TAB: for the years 2010 to 2012; RBA + TEF: for the years 2013 to 2018), it was reproduced the same procedure used for Region 1. And for Region 3, the remain Amazonia area, not covered by the vertical profile's regions of influence, were used the same concentrations minus bkg from Region 2. To compose the ΔVP for Amazonia it was produced the weighted mean for each height ΔCO_2 concentration considering the 3 regions and producing the weighted mean.

Carbon fluxes estimation

We used a column budget technique to estimate carbon total fluxes, which consists of the difference between CO_2 mole fraction measured in the vertical profile and the estimated background mole fraction (ΔCO_2) considering the travel time of air parcels along the trajectory from the coast to the site (eq. M1), following the methodology in Miller et al.[36], Gatti et al.[37], D'Amelio et al.[38], Gatti et al.[18], Basso et al.,[17,39] and Gatti et al.[4].

$$F_x = \int_{z=0(agl)}^{4.4km(asl)} \frac{\Delta X}{t(z)} dz$$

M1

To apply in eq. M1 we converted mole fractions [µmol CO_2 (mol dry air)$^{-1}$, i.e. ppm] to concentrations (mol CO_2 m^{-3}) using the density of air, where temperature (T) and pressure (P) were measured during the vertical profiles or and for situations where weren't, it were calculated T, P using the equation derived for temperature and pressure based in all measured T and P relating to height for each site[4]. To estimate the travel time t of air-masses from the coast to each sample site, we used back-trajectories for each altitude of the vertical profile, where 13-day backward trajectories are derived from the online version of the HYSPLIT model[40,41].

Our background mole fraction estimates were calculated according to the methodology described by Domingues et al.[42], using the geographical position of each air-mass back-trajectory when it intersects two virtual limits: 1) a latitude limit, from the Equator southwards at 30° W, and 2) a line from the Equator to the NOAA Global Monitoring Laboratory (NOAA/GML) observation site at Ragged Point, Barbados (RPB). Based on the atmospheric air circulation pattern over Amazonia we could relate the position where an air mass crosses the virtual line with the concentrations measured at remote sites in the Atlantic—RPB, Ascension Island, UK (ASC) and Cape Point, South Africa (CPT)—from NOAA/GML to determine the background[42].

Carbon fire fluxes were estimated based on eq. M2, where FCO is the total CO flux and is calculated identically to CO_2 fluxes according to eq. M1; and to isolate the CO from biomass burning process, we subtract the 'natural' CO flux from the total CO flux. $FCO_{natural}$, arising from direct soil CO emissions, and mainly CO from oxidation of volatile organic compounds (VOCs), such as isoprene that is emitted from the forest according to the methodology described at Gatti et al.[4]. We also used fire emission ratios calculated by site ($CO:CO_2$, in units of parts per billion-ppb CO per ppm CO_2) from measured CO concentrations from clearly identifiable plumes in the VPs during the dry season (ALF $CO:CO_2$ = 53.4 ± 9.9 (1σ variability); SAN $CO:CO_2$ = 55.5 ± 14.7; RBA $CO:CO_2$ = 73.2 ± 15.1; and TAB_TEF $CO:CO_2$ = 71.6 ± 17.2 ppbCO : ppmCO_2[4]. NBE represents the result of emissions and uptake from all processes in the influenced area for a specific VP, monthly and annual mean, excluding fire C emissions (NBE = total − fire).

$$FC_{Fire} = R_{CO_2:CO} \left(F_{CO} - F_{CO}^{Natural} \right)$$

M2

To scale for the whole Amazonia carbon fluxes was applied the same procedure as for Amazonia ΔVP and described in eq. 3 and 4.

$$FC_{region1} = \frac{(FC_{SAN} * Area_{SAN}) + (FC_{ALF} * Area_{ALF})}{Area_{SAN} + Area_{ALF}}$$

M3

$$Balance_{Am.} = \left(FC_{reg.1} * Area_{reg.1}\right) + \left(FC_{reg.2} * Area_{reg.2-reg.1}\right) + \left(FC_{reg.2} * Area_{reg.3}\right)$$

M4

Fluxes Uncertainty Analysis by Monte Carlo error propagation

We estimated our fluxes uncertainties by error propagation with Monte Carlo randomization with 1000 iterations, considering the uncertainty in the background concentration and in the air parcel travel time, and for separation of total fluxes in fire and land vegetation fluxes unrelated to fire, we account for the uncertainty in ratio of $CO:CO_2$ and in CO fluxes. The uncertainty due to CO_2 measurement uncertainty (<0.1 ppm) is negligibly small. For background uncertainties we consider that mole fraction uncertainties from ASC, CPT and RPB come from the standard deviation of the residuals to curve fits to CO_2. For back-trajectories and for separation of total fluxes in fire and land vegetation fluxes unrelated to fire uncertainties, we used a similar methodology described at Gatti et al.[4]. We estimate back-trajectory uncertainties based on the largest difference in mean profile travel time from HYSPLIT and two additional models, the FLEXPART Lagrangian particle dispersion model[43] and the mesoscale model BRAMS[44], for all profiles of 2010 using the RMSE values. For fluxes from fire, we use the standard deviation of emission ratios at each site and account for the CO flux uncertainties (estimated as for the CO_2 fluxes), and consider the uncertainty in natural CO flux of 25%. We calculate the annual mean uncertainties for the whole period as eq. M5 to be conservative, allowing for significant year to year correlation, where n is the number of years.

$$sigma = \frac{\sum sigma_i}{n} \quad \text{M5}$$

Additional source of uncertainty is the sampling height limitation to 4.4 km. Along the way of air masses trajectory that can vary from 2 to 9 days mean time until to the sampling sites, convective process can represent loss of carbon sources and sink surface contributions. Comparing the background concentration and the top of vertical profiles is one way to verify the possible loss of information. Supplementary Fig. 4 show the seasonal dispersion along the time series for the differences between the top of VP (>3.8 to 4.4 km) and the background. According to the method we use, the flux is obtained by the difference between of the measured CO_2 concentration in the VP and the background concentration and considering the travel time in the integration. Observing the Supplementary Fig. 4 it is clear that during the dry season is the period in which the loss of information is larger to positive (VP > bkg), because during burning season (peak of dry season) the top of VP starts with higher CO_2 and CO concentration due to convective processes promoted by biomass burning.

Another possible source of uncertainty is related to moisture in the samples. NOAA/GML have found that CO_2 concentration is artificially reduced when air samples with high (> 1.7%) water vapor are pressurized in PFP flasks to 2.7 bar, as a result of condensation[45]. A preliminary study using vertical profiles near Manaus (Amazonas state) compared PFP samples measured for CO_2 at LAGEE to onboard measurements from a trace gas flight analyser largely immune to water effects (Picarro model G2401-m) and found depletions in PFP CO_2 similar to those from the Baier et al study. This influence is likely greater near the surface, as humidity increases at lower altitudes. Thus, true CO_2 in the lower half of the profiles may be higher than measured, meaning that current fluxes could be underestimated (either too much sink or not enough source). However, because there are no known trends in absolute humidity between the two periods (2010-18 and 2019-2020), these sampling artifacts are unlikely to significantly affect the contrast in CO_2 fluxes we observe over time.

Missing data imputation

The missForest algorithm was applied to fill in the missing data for total and Fire C monthly fluxes at ALF, SAN, RBA and TABTEF sites, which occurred due to sampling and laboratory logistics issues. This non-parametric missing value imputation algorithm is based on the random forest methodology[46,47] and was implemented in R language[48] using the missForest package[49]. The known monthly data were used to adjust the missForest parameters (number of iterations, number of trees, number of variables randomly sampled in each division and others) for each site. Monthly variables (temperature, precipitation, burned area, EVI, GRACE and VPD) were used in the imputation method for total C flux (FC_{Total}) and fire C flux (FC_{Fire})[4]. These calculations were performed 1000 times, and the results are incorporated in the mean values for the missing months (Supplementary Fig. 5). The normalized RMSE was less than 0.0045 for all sites and fluxes. The RMSE values were 0.0041, 0.0060, 0.0027 and 0.0021 gC m^{-2} d^{-1} for total fluxes and 0.0008, 0.0019, 0.0004 and 0.0001 gC m^{-2} d^{-1} for fire fluxes in ALF, SAN, RBA and TAB_TEF, respectively. NBE missing data was obtained subtracting the Fire C fluxes from the Total C Fluxes. These RMSE values were used in the uncertainty calculation for the months with missing fluxes.

Regions of influence

We define regions of influence as those areas covered by the density of back-trajectories integrated over all vertical profiles and altitudes (up to 3500 m) for each site integrated on an annual (Extended data Fig. 1a) and a quarterly basis (Supplementary Fig. 6)[4,50]. Here we used the same regions of influence from Gatti et al.[4], for the period between 2010-18, and were calculated new areas for 2019 and 2020, which were estimated using Hysplit trajectory model[41,51] to calculated individual back-trajectories for each sample for each vertical profile and all flights between 2010 and 2018 at a resolution of 1 hour using 1˚x1˚ Global Data Assimilation System (GDAS) meteorological data. For each site, all the back-trajectories in a quarter (January-March, April-June, July-September, October-December) or annually were binned, and the number of instances (at hourly resolution) that the back-trajectories passed over a 1˚x1˚ grid cell was counted to determine the trajectory density in each grid cell up to an altitude of 3,500 m a.s.l.. In the annual regions of influence were excluded the grid cells with the lowest 2.5% trajectory density distribution. The mean annual regions of influence were determined by averaging the nine annual regions of influence for each site, by the sum of the number of points (frequency) within each grid cell integrating all vertical profiles in the year and then averaging all nine years[50].

Precipitation, temperature, GRACE, EVI, burned area and VPD data

We used the quarterly regions of influence maps as spatial weighting functions for all studied parameters to determine how each parameter influenced the carbon flux, following Gatti et al.[4] We used the databased GPCP (http://eagle1.umd.edu/GPCP_ICDR/GPCP_Monthly.html), version 1.3 for precipitation analysis (described by Huffman et al.[52]), which contains daily data since 1996 with a resolution of 1° × 1° latitude–longitude.

For temperature we used 2-m temperatures from ERA-5 that are monthly means of daily means since 1959 and were used with a resolution of 0.25° × 0.25° latitude–longitude, obtained from the European Centre for Medium-Range Weather Forecasts (ECMWF; https://cds.climate.copernicus.eu/cdsapp#!/dataset/reanalysis-era5-single-levels-monthly-means?tab=overview)[53].

We used the gridded monthly global water storage/height anomalies (equivalent water thickness) relative to a time-mean, derived from GRACE (Gravity Recovery and Climate Experiment) and GRACE-FO and processed at JPL (Jet Propulsion Laboratory) using the Mascon approach (Version2/RL06), with 0.5° × 0.5° resolution[54,55].

The VPD product is a measure of the indirect vapour pressure deficit in kPa (resolution of 2.5 arc-minute) of monthly means of temperature and humidity, provided by Climatic Research Unit (CRU) CRU Ts4.0[56]. The dataset was resampled to a 1°x1° spatial resolution using the monthly mean.

Evaluation of burned area was obtained from the Moderate Resolution Imaging Spectroradiometer (MODIS) Collection 6 MCD64A1 burned area product[57]. Collection 6 provides monthly tiles of burned area with 500 m spatial resolution over the globe. The algorithm uses several parameters for detecting burned area from the Terra and Aqua satellite products, including daily active fire (MOD14A1 and Aqua MYD14A1), daily surface reflectance (MOD09GHK and MYD09GHK), and annual land cover (MCD12Q1)[58–60]. The burned area product was resampled to 1x1° spatial resolution.

The Enhanced Vegetation Index (EVI) is a vegetation index that aims to highlight the fraction of photosynthetically active radiation (fPAR) from terrestrial vegetation targets. In general, high positive values show a higher proportion of fPAR, and therefore, greater biomass. The EVI product used was the MANVI: MODIS multiangle implementation of atmospheric correction (MAIAC) nadir-solar adjusted vegetation indices for South America, generated by in spatial resolution of 1 km and temporal resolution of 16 days[61].

Validation of temperature data The ERA5 was validated using thirty-five automatic meteorological field stations for temperature data from the INMET (National Institute of Meteorology, Brazil), covering the period between 1979 and 2018, respectively. In our study, the least-squares regression analysis was carried out by using the ERA5 data as the dependent variable and the automatic meteorological field stations as the independent variable. The ERA5 dataset explained 49 to 98% of the temperature variability captured by the automatic meteorological field stations. The RMSE varied ±0.4˚C to ±1.84 ˚C (see Supplementary Fig. 7).

Deforestation

The procedures to retrieve deforestation as a geographic data built by PRODES/INPE[27] based on historical series of LandSat images provides deforestation annual increments in the Brazilian Amazon. Detailed information of PRODES methodology is available and can be accessed[15]. We adopted the data period between 2010 and 2020. Using QGIS software it was generated a grid cell of 0.25° x 0.25° for the entire Brazilian Amazon which was filled with absolute values of deforested area of deforestation calculated for each cell and in each year of the series. The mean area of deforestation was calculated for the period within 2010-2018 inside each grid's cell. Absolute annual deforestation for 2019 and 2020 were also calculated with the same methodology. Both, the mean or the absolute values of deforestation were calculated in each study site of the measured VPs considering the sum of all cell values completely enclosed in each site.

Fire spots

Fire spots in Pan-Amazonia between 2010 and 2020 and burned area in Brazil´s Amazon were retrieved from INPES´s "Queimadas" wildfire monitoring program[16]. The number of fire spots detected per year in the grid cells and the overall means were calculated for each study site using QGIS software. "Fire spots" refer to fire pixels detected in the daily afternoon images of the MODIS sensor on board the AQUA NASA satellite since 2002 using the "Collection 6" algorithm that provides world-wide coverage of active vegetation fires[62–64]. Fire spots represent an under sampling of the actual fire extent in the vegetation since the monitoring miss most understory low-temperature fires as well as those occurring under cloudy skies and between consecutive satellite overpasses. However, relying on a stable sensor and proven algorithms, the data is an excellent indicator of temporal and spatial tendencies of fire occurrences[62]. The procedures to retrieve fire spots from Queimadas Project (INPE) between 2010 and 2020. The absolute number of fire spots registered per year between 2010 and 2020 was calculated in each study site, using QGIS software. Also, it was calculated the mean values of fire spots in the period between 2010 and 2018 in each study site.

Environmental law enforcement and accountability for illegal deforestation. We set up and systematized a comprehensive database for the Amazon encompassing all available records of infractions notices and administrative judgments between 2010 and 2020. IBAMA field inspection and judgments data between 2010 and 2020 were obtained from the Brazilian Open Data Portal (https://dados.gov.br/dataset?q=ibama, downloaded on 09/07/21). We removed duplicate records by applying a composite primary key encompassing the columns *"seq_auto_infracao", "num_auto", "ser_auto", "cpf_cnpj", "valor_auto", "quant_area" and "num_processo"* and filtered data for the states of the Legal Amazon: Acre, Amapá, Amazonas, Pará, Rondônia, Roraima, Tocantins, and Mato Grosso and Maranhão. We used only infraction notices and fines related to crimes against the flora (basically illegal deforestation but also other forms of native vegetation suppression and associated crimes).

Data Availability Statement Additional data (2019 and 2020) will be available at PANGAEA. Data submission 2022-08-22T13:10:00Z (Luciana V. Gatti, Instituto Nacional de Pesquisas Espaciais), PDI-32629.

34. Eva, H. *et al.* *a Proposal for Defining the Geographical*. *A proposal for defining the geographical boundaries of Amazonia* (2005). doi:ISBN 9279000128
35. Olson, D. M. *et al.* Terrestrial Ecoregions of the World: A New Map of Life on Earth. *Bioscience* (2001). doi:10.1641/0006-3568(2001)051[0933:teotwa]2.0.co;2
36. Miller, J. B. *et al.* Airborne measurements indicate large methane emissions from the eastern Amazon basin. *Geophys. Res. Lett.* **34**, (2007).
37. Gatti, L. V. *et al.* Vertical profiles of CO2 above eastern Amazonia suggest a net carbon flux to the atmosphere and balanced biosphere between 2000 and 2009. *Tellus, Ser. B Chem. Phys. Meteorol.* (2010). doi:10.1111/j.1600-0889.2010.00484.x
38. D'Amelio, M. T. S., Gatti, L. V., Miller, J. B. & Tans, P. Regional N2O fluxes in Amazonia derived from aircraft vertical profiles. *Atmos. Chem. Phys.* **9**, 8785–8797 (2009).
39. Basso, L. S. *et al.* Seasonality and interannual variability of CH 4 fluxes from the eastern Amazon Basin inferred from atmospheric mole fraction profiles. *J. Geophys. Res. Atmos.* **121**, 168–184 (2016).
40. Draxler, R. R. & Rolph, G. D. HYSPLIT (HYbrid Single-Particle Lagrangian Integrated Trajectory). *NOAA Air Resour. Lab. Coll. Park. MD* (2003).
41. Stein, A. F. *et al.* NOAA's HYSPLIT Atmospheric Transport and Dispersion Modeling System. *Bull. Am. Meteorol. Soc.* **96**, 2059–2077 (2015).
42. Domingues, L. G. *et al.* A new background method for greenhouse gases flux calculation based in back-trajectories over the Amazon. *Atmosphere (Basel).* **11**, (2020).
43. Stohl, A., Forster, C., Frank, A., Seibert, P. & Wotawa, G. Technical note: The Lagrangian particle dispersion model FLEXPART version 6.2. *Atmos. Chem. Phys.* **5**, 2461–2474 (2005).

44. Freitas, S. R. *et al.* The Coupled Aerosol and Tracer Transport model to the Brazilian developments on the Regional Atmospheric Modeling System (CATT-BRAMS) – Part 1: Model description and evaluation. *Atmos. Chem. Phys.* **9**, 2843–2861 (2009).
45. Baier, B. C. *et al.* Multispecies Assessment of Factors Influencing Regional CO 2 and CH 4 Enhancements During the Winter 2017 ACT-America Campaign. *J. Geophys. Res. Atmos.* **125**, (2020).
46. Jiang, N. & Riley, M. L. Exploring the Utility of the Random Forest Method for Forecasting Ozone Pollution in SYDNEY. *J. Environ. Prot. Sustain. Dev.* **1**, 245–254 (2015).
47. Stekhoven, D. J. & Buhlmann, P. MissForest--non-parametric missing value imputation for mixed-type data. *Bioinformatics* **28**, 112–118 (2012).
48. R Core Team. R: A language and environment for statistical computing. *R: Foundation for Statistical Computing* (2020). Available at: https://www.r-project.org.
49. Stekhoven, D. J. missForest: Nonparametric Missing Value Imputation using Random Forest. R package version 1.4. (2013).
50. Cassol, H. L. G. *et al.* Determination of Region of Influence Obtained by Aircraft Vertical Profiles Using the Density of Trajectories from the HYSPLIT Model. *Atmosphere (Basel).* **11**, 1073 (2020).
51. Rolph, G., Stein, A. & Stunder, B. Real-time Environmental Applications and Display sYstem: READY. *Environ. Model. Softw.* **95**, 210–228 (2017).
52. Huffman, G. J. *et al.* Global Precipitation at One-Degree Daily Resolution from Multisatellite Observations. *J. Hydrometeorol.* **2**, 36–50 (2001).
53. Hersbach, H. *et al.* The ERA5 global reanalysis. *Q. J. R. Meteorol. Soc.* **146**, 1999–2049 (2020).
54. Watkins, M. M., Wiese, D. N., Yuan, D.-N., Boening, C. & Landerer, F. W. Improved methods for observing Earth's time variable mass distribution with GRACE using spherical cap mascons. *J. Geophys. Res. Solid Earth* **120**, 2648–2671 (2015).
55. D. N. Wiese, D.-N. Yuan, C. Boening, F. W. Landerer, M. M. W. JPL GRACE Mascon Ocean, Ice, and Hydrology Equivalent Water Height RL06 CRI Filtered Version 02. (2022). doi:doi.org/10.5067/TEMSC-3JC62
56. Abatzoglou, J. T., Dobrowski, S. Z., Parks, S. A. & Hegewisch, K. C. TerraClimate, a high-resolution global dataset of monthly climate and climatic water balance from 1958–2015. *Sci. Data* **5**, 170191 (2018).
57. Giglio, L., Boschetti, L., Roy, D. P., Humber, M. L. & Justice, C. O. The Collection 6

MODIS burned area mapping algorithm and product. *Remote Sens. Environ.* **217**, 72–85 (2018).

58. Vermote, E. F., El Saleous, N. Z. & Justice, C. O. Atmospheric correction of MODIS data in the visible to middle infrared: first results. *Remote Sens. Environ.* **83**, 97–111 (2002).
59. Justice, C. . *et al.* An overview of MODIS Land data processing and product status. *Remote Sens. Environ.* **83**, 3–15 (2002).
60. Friedl, M. A. *et al.* MODIS Collection 5 global land cover: Algorithm refinements and characterization of new datasets. *Remote Sens. Environ.* **114**, 168–182 (2010).
61. Dalagnol, R; Wagner, FH; Galvão, LS; Oliveira, LE; Aragao, C. *The MANVI product: MODIS (MAIAC) nadir-solar adjusted vegetation indices (EVI and NDVI) for South America*. (2019). doi:10.5281/zenodo.3159488
62. Wooster, M. J. *et al.* Satellite remote sensing of active fires: History and current status, applications and future requirements. *Remote Sens. Environ.* **267**, 112694 (2021).
63. Setzer, A.W.; Ferreira, N.J.; Morelli, F. Cap. 01, Queimadas e Incêndios Florestais: Mediante Monitoramento Orbital. in *Programa Queimadas do INPE* (2021).
64. Implementation, F. M. and M. GOFC/GOLD Global Observation of Forest Cover/Global Observation of Landcover Dynamics Fire Programme. Available at: https://gofcgold.org/.

Supplementary Files

This is a list of supplementary files associated with this preprint. Click to download.

- ExtendeddataSupplementaryInformationfile.pdf